R. Renner, J. Beerten, D. Van Hertem, “Optimal dc reference voltage in HVDC grids,” *Proc. IET International Conference on AC and DC Power Transmission ACDC 2015*, 11th ed., Birmingham, UK, Feb. 10–12, 2015, 6 pages.

Digital Object Identifier: 10.1049/cp.2015.0067

URL (IET Digital Library):
http://digital-library.theiet.org/content/conferences/10.1049/cp.2015.0067

URL (IEEE Xplore Digital Library):
http://ieeexplore.ieee.org/xpl/articleDetails.jsp?arnumber=7140601

OPTIMAL DC REFERENCE VOLTAGE IN HVDC GRIDS

R. H. Renner*, J. Beerten*,†, D. Van Hertem*
robert.renner@esat.kuleuven.be, jef.beerten@esat.kuleuven.be, dirk.vanhertem@esat.kuleuven.be
* KU Leuven, Belgium,
† NTNU, Norway

Abstract

In a HVDC grid, power energy equilibrium must be guaranteed at every moment to prevent DC voltage to increase or decrease to unacceptable values. Contrary to the frequency in an AC power system, the DC voltage cannot be assumed to be the same throughout the system, since a DC voltage difference is necessary to have a current flow. To operate HVDC grids as far as possible from DC voltage stability limits, the selection of the DC reference voltage and DC reference node are crucial factors. This paper introduces a method to find the optimal DC voltage in a HVDC grid based on power flow and line resistances. The method is implemented in the open-source software MatACDC and the results are verified by dynamic simulations in DIgSILENT, using a one area DC voltage restoration controller. **Keywords:** HVDC grid, Power System Operation, Security of Supply, DC Voltage

1 Introduction

In the 1990's, Europe started to change the power system from vertically integrated monopoly utilities to a liberalised system in order to increase the efficiency of the power system and, at the same time, increase the generation from sustainable sources. These changes must not jeopardies the reliability of the power system [1]. For the next years, an increase of the generation from sustainable sources from 12.7% in 2010 [2] to 20 % in 2020 [3] is planned. Sustainable generation has the limitation that the power plants have to be built where the primary energy is available and that the electrical energy is available when the primary energy is available [4]. This results in longer transmission distances and a need for storage. As, at the moment, the only efficient storage system for electrical energy are pumped storage power plants [5] which are connected to geographical certainties, the idea of an European super grid was developed [6]. This, could be built using HVDC technology and connect wind generation, located offshore or onshore, photovoltaic power plants in southern Europe, pumped storage in Scandinavia and the Alps and load centres in central Europe. The reasons to select HVDC are lower losses for long distance transmission and the absence of reactive power [7], [8]. If HVDC grids arise, they have to fulfil the same reliability standards as the connected AC power system.

The indicator for the energy equilibrium in HVDC grids is the DC voltage. It increases if more energy is going into the system than what is going out (accounting for the losses), because the imbalance is stored in the capacitances of the HVDC grid. Similarly, it decreases if more energy is going out of the system than what is going into it, because the imbalance is supplied by the energy stored in the capacitances of the HVDC grid. Thus, the DC voltages will float due to changing injections and possible outages. From a system operation perspective, it is therefore beneficial to keep the DC voltage margin to respectively the upper and lower DC voltage limit as large as possible.

A first solution to set up the DC voltage reference points in the HVDC grid is presented in [9], where the objective is to change the DC voltage in the system by changing the powers as little as possible amongst all nodes, in order to get an average DC voltage of 1 pu. The result is not necessarily an optimum, with respect to the DC voltages margins as argued above, nor does it minimise the losses. In [10] is the objective to decrease the losses of the HVDC grid by changing the DC voltage set-points. Consequentially it results in a DC voltage level that is as high as possible and thus a reduced upper DC voltage margin.

This paper aims at addressing the shortcomings in the methods found in literature by presenting an optimal DC voltage reference selection procedure, that maximises the energy stored in both upward and downward voltage control bands. To do so, this paper starts with giving an introduction to reliability in transmission systems and possible changes if HVDC grids arise. This is followed by DC voltage behaviour in HVDC grids and a section that explains the algorithm to find an as large as possible gap to the DC voltage limits with given power set-points. It contains a section that explains a case study and compares the results with results from DIgSILENT and closes with a conclusion.

2 Reliability in transmission systems

Reliability in transmission systems depends mainly on the compliance of a security state, e.g N-1, and the balance of generation and load. With a possible arise of HVDC grids, additionally to the existing AC power systems, different combinations for the security state as well as the balancing reserve can be defined. Figure 1 shows the different types of combination, for both security state and balancing reserve. It may be that the security state is defined for AC power system and HVDC grid together and that both use the same balancing reserve. Another option is, that each system defines a security state and balancing reserve, but for defined regions the security state/balancing reserve of one system is overlapping with the other. An example could be the primary reserve, which could be the same for both systems. And the last possibility is that both systems have to fulfil their own security state and have to provide their own reserves. As the security state and the balancing reserves are not dependent of each other, all combinations are possible.

No matter how the reserve is organised, an indicator for an unbalance in AC power systems is the frequency. Every unbalance

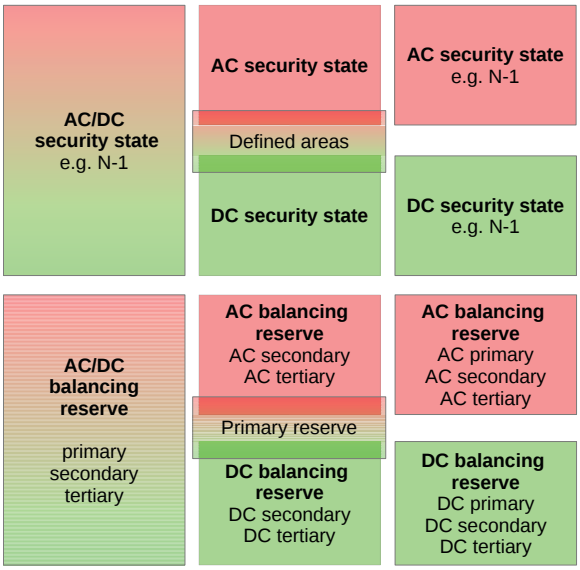

Figure 1: From left to right: The same security state/balance reserve for both systems, a split security state/balance reserve but with well defined overlapping, independent security state/balance reserve

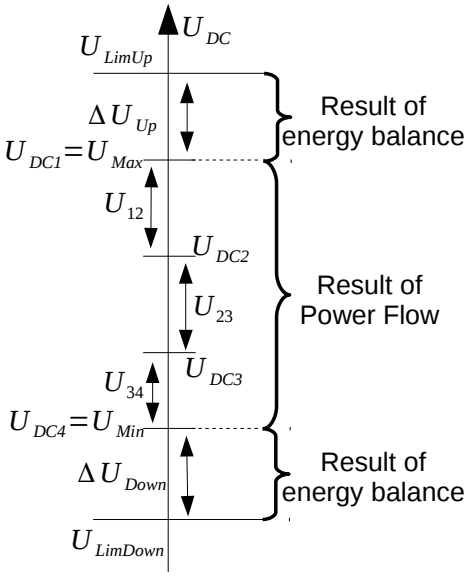

Figure 2: Used DC voltage band and available distance to the upper and lower limit

is stored in or withdrawn from the energy of the rotating masses. If more energy is generated then consumed, the frequency will start to increase and if less energy is generated then consumed, the frequency will decrease. The frequency can be assumed to be constant over the entire AC system, meaning that an energy imbalance can be observed in the entire system. In order to have time to react to an unbalance, the frequency should stay as close to its reference value as possible. Maintaining the band to the stability borders as large as possible [11]. In HVDC grids the indicator for the energy balance is the DC voltage.

3 DC voltage in HVDC grids

Contrary to frequency in AC power systems, DC voltage in HVDC grids cannot be assumed equal in all nodes of the HVDC grid. This is since in HVDC grids, two effects are influencing the DC voltage distribution: the power flow [9] and the energy balance [12]. The steady state power flow equation is

$$\mathbf{P} = \mathbf{U} \circ \mathbf{I} = \mathbf{U} \circ \mathbf{GU} \tag{1}$$

with P the power injection vector, U the node voltage vector, I the current injection vector and G the conductance matrix. The result is a DC voltage distribution as it is shown in figure 2 for a four node system. The DC voltage difference between the nodes is defined by the power flow, the resistances between the nodes and the position between the DC voltage limits. Figure 3 shows the dependency of the highest and lowest nodal voltage, for the HVDC grid described in section 5 and the data available in appendix. From figure 3 follows a gradient $m = \frac{\Delta U_{Min}}{\Delta U_{Max}} \approx \frac{0.11pu}{0.105pu} = 1.05$. Thus, for a first approach the gradient can assumed to be 1. This would mean, that a DC voltage shift at one node would result in the same DC voltage shift for all nodes. Then, the band between U_{Max} and U_{Min} can assumed to be

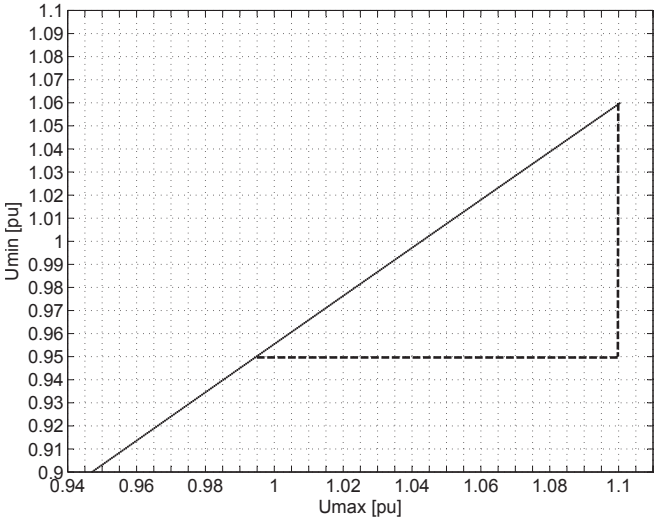

Figure 3: Plot of U_{Max} and U_{Min} for the HVDC grid described in section 5 between the limits of $1.1pu$ and $0.9pu$, and the triangle (dotted lines) used to calculate the gradient

fixed for a given power flow pattern and hence the corresponding converter power set-points. Furthermore, the DC voltage is an indicator for the energy balance. The instantaneous power is expressed as

$$P(t) = i(t) \cdot u(t). \tag{2}$$

For a lossless capacitor this becomes

$$P(t) = C \cdot \frac{du(t)}{dt} \cdot u(t). \tag{3}$$

With the energy written as the integral of the power

$$E = \int_{t_1}^{t_2} P(t)dt, \tag{4}$$

expression (3) becomes

$$\int_{t_1}^{t_2} P(t)dt = \int_{t_1}^{t_2} \left(C \cdot \frac{du(t)}{dt} \right) \cdot u(t)dt \quad (5)$$

$$\Rightarrow P(t_2) \cdot t_2 - P(t_1) \cdot t_1 = \frac{1}{2} \cdot C \cdot (u(t_2)^2 - u(t_1)^2) \quad (6)$$

If the system consists of n nodes with a capacitance C_j, controllable power injection P_j and a DC voltage u_i with $1 \leq i \leq n$ follows

$$\sum_{j=1}^{n} P_j(t_2) \cdot t_2 - \sum_{j=1}^{n} P_j(t_1) \cdot t_1 = \frac{1}{2} \cdot \sum_{j=1}^{n} C_j \cdot (u_i(t_2)^2 - u_i(t_1)^2) \quad (7)$$

Assuming no power imbalance at moment t_1

$$\sum_{j=1}^{n} P_j(t_1) = 0 \quad (8)$$

When we assume that the maximal DC voltage in the HVDC grid is U_{Max} and that the upper limit is U_{LimUp}, this results in

$$\sum_{j=1}^{n} P_j(t_2) \cdot t_2 = E_{BufferUp} \quad (9)$$

$$\Rightarrow E_{BufferUp} \approx \frac{1}{2} \cdot \sum_{j=1}^{n} C_j \cdot (U_{LimUp}^2 - U_{Max}^2) \quad (10)$$

To get an optimal stability, the objective is to maximise upper and lower buffer energy.

4 Optimisation

The system stability is in danger if the upper or lower DC voltage limit is reached. Thus, a maximal band between scheduled operation points and defined limits is beneficial. Equation (10) shows that the buffer energy depends on the voltages for a given power flow. From figure 2 follows then, that the overall buffer energy is maximal, if ΔU_{Up} and ΔU_{Down} are equal.
Mathematically, the behaviour of two DC voltages for a given power flow can be approximated as a linear function with a gradient equal to 1 (figure 3). Then, the DC voltage difference between two nodes is defined by the power flow (equation (9)) and thus, can assumed to be constant for the energy balance equations. This results in:

$$U_{Max} = m \cdot U_{Min} + d \quad (11)$$

with U_{Max} the highest DC voltage, U_{Min} the lowest DC voltage, m the gradient equal to 1 and d = $U_{Max} - U_{Min}$. With the constraint:

$$\Delta U_{Up} = \Delta U_{Down} \quad (12)$$

one gets

$$U_{Min}^{ref} = \frac{U_{LimUp} - d + U_{LimDow}}{m + 1} \quad (13)$$

$$U_{Max}^{ref} = \frac{U_{LimUp} + d + U_{LimDow}}{m + 1} \quad (14)$$

The result is the DC voltage set-point at either the node with lowest/highest DC voltage. It may be that this is not the best choice for the DC reference node, as it could be poorly connected to the rest of the system and hence could not be available after e.g. a line outage.
Anyway, this optimisation is embedded in the open-source software MatACDC [13, 14], that can calculate an ACDC power flows. It may be that the approximation does not give acceptable results and a second iteration is necessary. Therefore, an exit condition has to be defined. This can be the difference Z between ΔU_{Up} and ΔU_{Down}, which should be below a predefined margin. The flow chart for the optimisation algorithm is shown in figure 4. Starting from a defined power flow, the exit condition is checked. If $\mid \Delta U_{Up} \mid - \mid \Delta U_{Down} \mid < Z$, the output is the DC voltage for all nodes. If not, the DC voltage set-point for the node with the lowest DC voltage is calculated (equation (13)). This voltage is used as DC voltage set-point for the following power flow calculation. The exit condition is checked for the new DC voltages $\mid \Delta U_{Up}^{new} \mid - \mid \Delta U_{Down}^{new} \mid < Z$, etc. If droop control is influencing any of this steps, it has to be compensated as it will change the results.

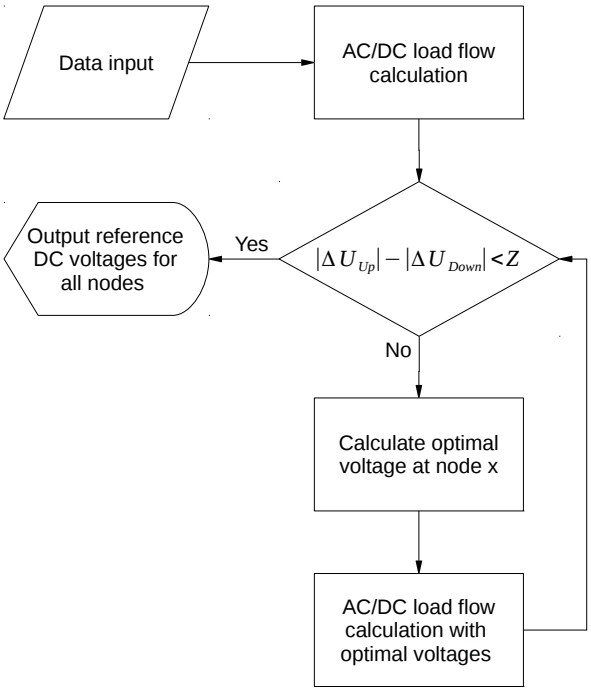

Figure 4: Flow chart of optimal DC voltage calculation

5 Case study

As a test system we choose the planned HVDC connections in Germany [15] and connect them to get a HVDC grid. Figure 5 shows the HVDC grid as purple connections. The HVDC connections are divided in planned connections (darker purple with slant segments) and added ones (lighter purple with straight segments). The planned ones are described in the grid development plan [15] and the added ones are implemented to build redundancies. The purple dots represent nodes with their dedicated number. Figure 5 also shows planned AC reinforcements. Figure 6 shows a schematic overview of the resulting HVDC grid without existing or planned AC lines. To simplify the implementation, the converter stations are assumed to be identical, with 1 GW rated active power. The distances between

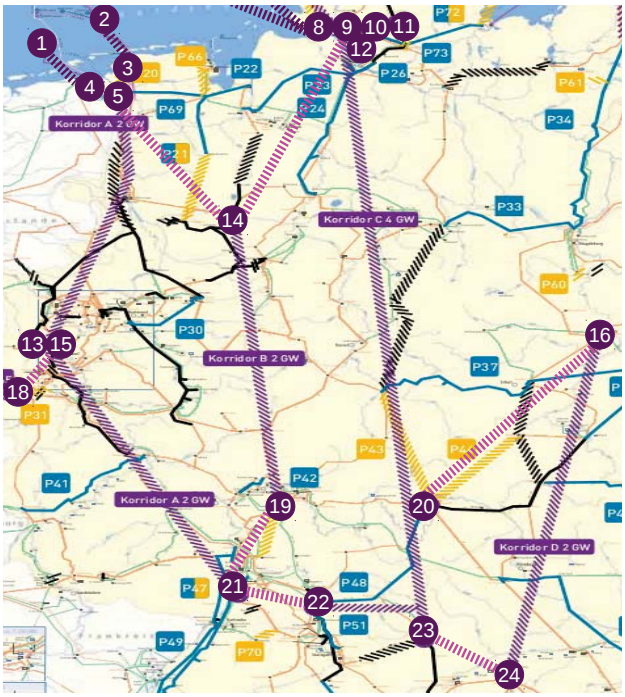

Figure 5: Development plans of the German TSOs [15] with some additional circuits (lighter purple with straight segments)

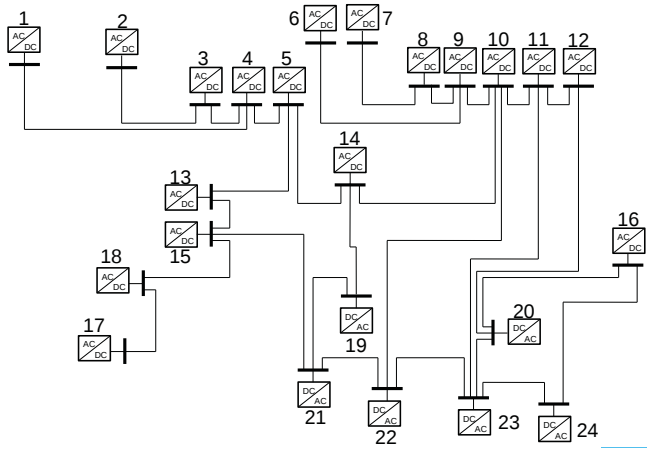

Figure 6: Schematic of the implemented case study HVDC grid

the nodes are either taken from [15] or estimated from the geographical distance. The result is a HVDC grid with 24 converter stations each with 1 GW, four connected wind farms with 4 GW connected off-shore wind power plants and around 3000 km transmission lines. The test case is a situation with a power flow from north to south, as a result of wind generation in the northern part. All parameters of the converters and lines can be found in the appendix.

For this HVDC grid, the optimal DC voltage is calculated with the steps from figure 4. The first power flow calculation gives a maximal DC voltage of $U_{DC6} = 1.0186pu$ at node 6 and a minimal DC voltage of $U_{DC17} = 0.9749pu$ at node 17. With DC voltage limits of $U_{LimUp} = 1.1pu$ and $U_{LimDow} = 0.9pu$ is $Z = 0.0065pu$. To get a better result, is with equation (13) a new DC reference voltage $U^{ref}_{DC17} = 0.9782pu$ calculated. Equation (14), would alternatively calculate the optimal DC reference voltage at node 6. It is also possible to define unsymmetrical limits, which would change the results. To get the new DC reference voltages for all nodes, another power flow calculation is performed. The result is a DC voltage profile as shown in figure 7. Each point is the DC voltage at one node, the corresponding DC voltages are listed in appendix table 2 and $Z = 0.0002pu$.

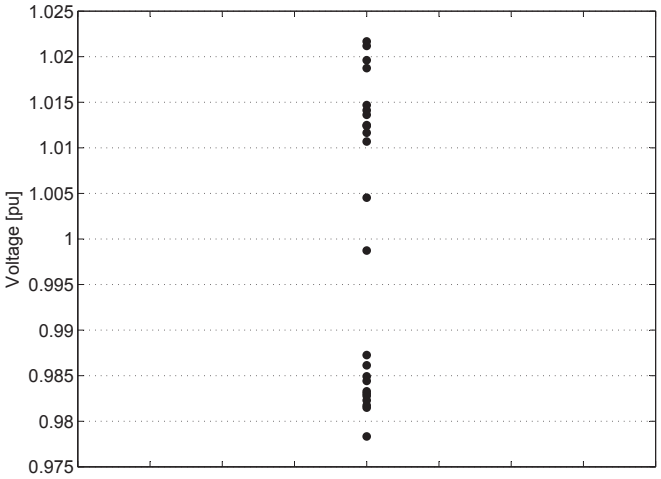

Figure 7: DC voltages of all nodes with optimal DC voltage distribution

To verify the results of the optimisation, the described grid is also implemented in DIgSILENT. To maintain the DC voltage in the grid and to choose an arbitrary node as reference, a one area decentralised DC voltage restoration controller is implemented. It maintains the DC voltage for the whole HVDC grid by calculating the power imbalance and sending it to participating converter stations, adding it to the power set-point. The controller has the structure shown in figure 8. Each node and each

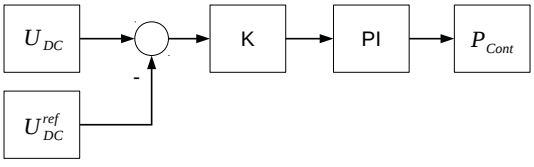

Figure 8: One area secondary controller

reference DC voltage can be used as input for the DC voltage restoration controller. It calculates the difference between the reference DC voltage and the actual DC voltage, multiplies it with the area droop to get the power imbalance provided by the droop control. This power imbalance is then eliminated with a PI-controller by sending the power mismatch to the participating

converters.
A comparison of the results of the dynamic simulation with DIgSILENT and the optimisation algorithmic is shown in figure 9. The first second, the system equalises minor differences

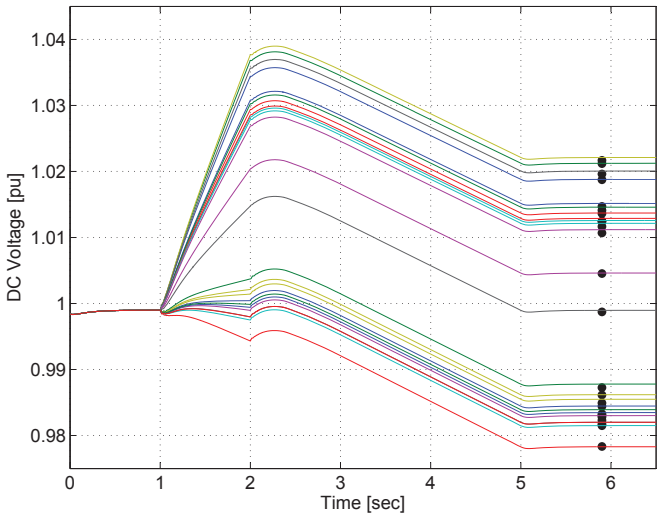

Figure 9: DC voltage for dynamic simulation and steady state (black dots) with optimal DC reference voltage

between the converter stations and the DC reference voltage is randomly set to $U_{DC17}^{ref} = 0.999pu$. From second one to second 2 the converter power set-points are established and from second 2 to second 5, the DC voltage is changed to get a similar DC voltage profile as in the steady state calculation. As DC voltage reference, node 6 is selected with the DC reference voltage of $U_{DC17}^{ref} = 0.9782pu$.
The differences in the DC voltages result from the fact that the losses are not equal and that the point of common coupling (PCC) is defined differently (see also power diagram in appendix figure 10): in the DIgSILENT simulations, the PCC is defined between the transformer and filters at the AC side, whereas in the steady state simulation the PCC is at the DC bus bar.

6 Conclusion

This work presents a calculation to find the optimal DC references voltage for a HVDC grid. To show that the optimisation is valid, a case study is implemented and the optimal DC reference voltages are calculated. These results are additionally compared with a simulation in DIgSILENT. Therefore a DC voltage controller was implemented to shift the DC voltages to the defined DC reference voltage. All these tests had sufficient results and showed that the method is able to calculate the optimal DC reference voltage. A drawback of the method is that the power flow has to be known to perform the calculation. Thus, is its application limited to scheduling tasks as changes in the topology and/or power of the converters will change the optimal DC reference voltage. This algorithm can be easily integrated in the DC SCADA/EMS as it would require limited communication.

7 Acknowledgement

The research leading to these results has received funding from the People Programme (Marie Curie Actions) of the European Union's Seventh Framework Programme FP7/2007-2013/ under REA grant agreement no. 317221, project title MEDOW.
Jef Beerten is funded by a postdoctoral research grant from the Research Foundation - Flanders (FWO).

8 Appendix

Converter Number	Power from AC to DC	DC voltage restoration control
1	$1000MW$	No
2	$1000MW$	No
3	$600MW$	No
4	$500MW$	No
5	$500MW$	No
6	$1000MW$	No
7	$1000MW$	No
8	$500MW$	No
9	$500MW$	No
10	$500MW$	Yes
11	$500MW$	No
12	$500MW$	No
13	$-800MW$	Yes
14	$-800MW$	No
15	$-800MW$	Yes
16	$500MW$	Yes
17	$-800MW$	No
18	$-500MW$	Yes
19	$-800MW$	No
20	$-800MW$	No
21	$-800MW$	No
22	$-800MW$	No
23	$-800MW$	No
24	$-800MW$	No

Table 1: Converter power set-points

Node Number	DC Voltage
1	$1.0186pu$
2	$1.0211pu$
3	$1.0135pu$
4	$1.0124pu$
5	$1.0044pu$
6	$1.0216pu$
7	$1.0195pu$
8	$1.0146pu$
9	$1.0140pu$
10	$1.0123pu$
11	$1.0115pu$
12	$1.0106pu$
13	$0.9860pu$
14	$0.9986pu$
15	$0.9843pu$
16	$0.9872pu$
17	$0.9782pu$
18	$0.9813pu$
19	$0.9827pu$
20	$0.9848pu$
21	$0.9816pu$
22	$0.9829pu$
23	$0.9832pu$
24	$0.9822pu$

Table 2: Optimal DC voltage set-points

Nominal Voltage	Rated Power	Capacitance	Inductance
$\pm 600kV$	$1000MW$	$100\mu F$	$37.35mH$

Table 3: Converter parameter

Branch	R'	l	R	C'	C
1-4	$0.0139\frac{\Omega}{km}$	165 km	2.29Ω	$0.23\frac{\mu F}{km}$	$38.0\mu F$
2-3	$0.0139\frac{\Omega}{km}$	200 km	2.78Ω	$0.23\frac{\mu F}{km}$	$46.0\mu F$
3-4	$0.0139\frac{\Omega}{km}$	20 km	0.28Ω	$0.23\frac{\mu F}{km}$	$4.6\mu F$
4-5	$0.0139\frac{\Omega}{km}$	70 km	0.97Ω	$0.23\frac{\mu F}{km}$	$16.1\mu F$
5-14	$0.0139\frac{\Omega}{km}$	320 km	2.20Ω	$0.23\frac{\mu F}{km}$	$73.6\mu F$
5-13	$0.0139\frac{\Omega}{km}$	160 km	4.45Ω	$0.23\frac{\mu F}{km}$	$36.8\mu F$
6-9	$0.0139\frac{\Omega}{km}$	200 km	2.78Ω	$0.23\frac{\mu F}{km}$	$46.0\mu F$
7-8	$0.0139\frac{\Omega}{km}$	130 km	1.81Ω	$0.23\frac{\mu F}{km}$	$29.9\mu F$
8-9	$0.0139\frac{\Omega}{km}$	10 km	0.14Ω	$0.23\frac{\mu F}{km}$	$2.3\mu F$
9-10	$0.0139\frac{\Omega}{km}$	15 km	0.21Ω	$0.23\frac{\mu F}{km}$	$3.5\mu F$
10-11	$0.0139\frac{\Omega}{km}$	20 km	0.28Ω	$0.23\frac{\mu F}{km}$	$4.6\mu F$
10-22	$0.0139\frac{\Omega}{km}$	700 km	9.73Ω	$0.23\frac{\mu F}{km}$	$161.0\mu F$
11-12	$0.0139\frac{\Omega}{km}$	50 km	0.70Ω	$0.23\frac{\mu F}{km}$	$11.6\mu F$
12-20	$0.0139\frac{\Omega}{km}$	670 km	9.31Ω	$0.23\frac{\mu F}{km}$	$154.1\mu F$
13-15	$0.0139\frac{\Omega}{km}$	20 km	0.28Ω	$0.23\frac{\mu F}{km}$	$4.6\mu F$
14-19	$0.0139\frac{\Omega}{km}$	380 km	5.28Ω	$0.23\frac{\mu F}{km}$	$87.4\mu F$
16-24	$0.0139\frac{\Omega}{km}$	450 km	6.26Ω	$0.23\frac{\mu F}{km}$	$103.5\mu F$
21-19	$0.0139\frac{\Omega}{km}$	100 km	1.39Ω	$0.23\frac{\mu F}{km}$	$23.0\mu F$
21-22	$0.0139\frac{\Omega}{km}$	100 km	1.39Ω	$0.23\frac{\mu F}{km}$	$23.0\mu F$
15-18	$0.0139\frac{\Omega}{km}$	60 km	0.83Ω	$0.23\frac{\mu F}{km}$	$13.8\mu F$
15-21	$0.0139\frac{\Omega}{km}$	340 km	4.73Ω	$0.23\frac{\mu F}{km}$	$78.2\mu F$
17-18	$0.0139\frac{\Omega}{km}$	100 km	1.39Ω	$0.23\frac{\mu F}{km}$	$23.0\mu F$
23-24	$0.0139\frac{\Omega}{km}$	100 km	1.39Ω	$0.23\frac{\mu F}{km}$	$23.0\mu F$
16-20	$0.0139\frac{\Omega}{km}$	250 km	3.48Ω	$0.23\frac{\mu F}{km}$	$57.5\mu F$
20-23	$0.0139\frac{\Omega}{km}$	100 km	1.39Ω	$0.23\frac{\mu F}{km}$	$23.0\mu F$
22-23	$0.0139\frac{\Omega}{km}$	100 km	1.39Ω	$0.23\frac{\mu F}{km}$	$23.0\mu F$
23-24	$0.0139\frac{\Omega}{km}$	100 km	1.39Ω	$0.23\frac{\mu F}{km}$	$23.0\mu F$

Table 4: Line parameter one pole equivalent

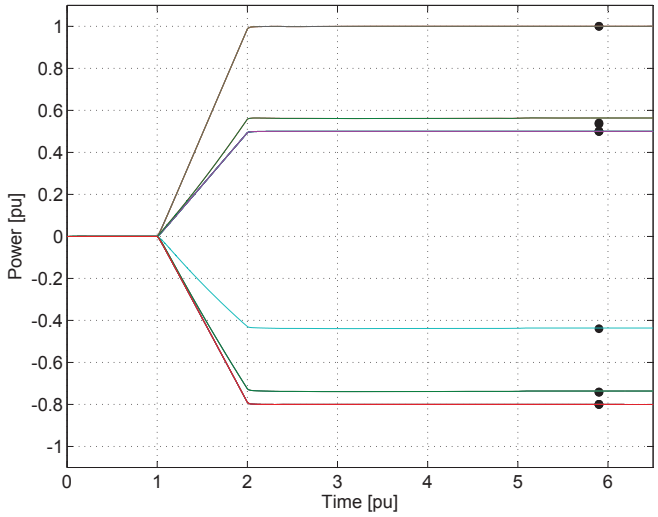

Figure 10: Power flow for dynamic and steady state (black dots) simulation with optimal DC reference voltage

References

[1] D. Kirschen and G. Strbac, *Fundamentals of Power System Economics* . John Wiley & Sons Ltd, 2004.

[2] "Renewable energy progress report," European Commission, 2013. [Online]. Available: http://eur-lex.europa.eu/legal-content/EN/ALL/?uri=CELEX:52013DC0175

[3] "Directive 2009/28/EC," European Commission, Apr. 2009. [Online]. Available: http://ec.europa.eu/energy/renewables/targets_en.htm

[4] T. Burton, D. Sharpe, N. Jenkins, and E. Bossanyi, *Wind Energy Handbook*. John Wiley & Sons, Ltd, 2001.

[5] D. Oeding and B. Oswald, *Elektrische Kraftwerke und Netze*, 6th ed. Springer-Verlag, 2004.

[6] H. Ergun, J. Beerten, and D. Van Hertem, " Building a new overlay grid for Europe ," in *Power and Energy Society General Meeting, 2012 IEEE* , 2012, pp. 1–8.

[7] J. Arrillaga, Y. Liu, and N. Watson, *Flexible Power Transmission*. John Wiley & Sons Ltd, 2007.

[8] D. Van Hertem and M. Ghandhari, "Multi-terminal VSC HVDC for the European supergrid: Obstacles," *Renewable and Sustainable Energy Reviews*, vol. 14, no. 9, pp. 3156–3163, Dec. 2010.

[9] J. Beerten, "Modeling and Control of DC Grids," Ph.D. dissertation, KU Leuven, May 2013.

[10] M. Aragüés-Peñalba, A. Egea-Àlvarez, O. Gomis-Bellmunt, and A. Sumper, "Optimum voltage control for loss minimization in HVDC multi-terminal transmission systems for large offshore wind farms," *Electric Power Systems Research*, vol. 89, pp. 54–63, Aug. 2012.

[11] "Operation Handbook," ENTSO-E, 2012. [Online]. Available: https://www.entsoe.eu/publications/system-operations-reports/operation-handbook

[12] B. R., *Elektrische Energie Boek 1*. Garant, 2002.

[13] J. Beerten and R. Belmans, "Development of an Open Source Power Flow Software for HVDC Grids and Hybrid AC/DC Systems: MatACDC," *IET Generation Transmission & Distribution*, 2014.

[14] J. Beerten, "MatACDC User's Manual ," 2012. [Online]. Available: http://www.esat.kuleuven.be/electa/teaching/matacdc/MatACDCManual

[15] O. Feix, R. Obermann, M. Strecker, and A. Brötel, "NETZENTWICKLUNGSPLAN STROM 2012 ," 2012. [Online]. Available: http://www.netzentwicklungsplan.de